Lattice Codes for Amplified Direct-Detection Optical Systems

Wei Mao and Joseph M. Kahn, *Fellow, IEEE*

***Abstract*—Theories of shaping for lattice codes have been developed for systems (optical or non-optical) using coherent detection with additive white Gaussian noise (AWGN) and for direct-detection optical systems with AWGN. This paper considers shaping for amplified direct-detection optical systems in which signal-spontaneous beat noise, a form of signal-dependent noise, is dominant. An *N*-dimensional (*N*-D) signal is formed by modulating the intensities (squares of field magnitudes) of a sequence of *N* time-disjoint pulses. In field magnitude coordinates, signal energy is represented by a L^2 norm, and the optimal constellation bounding region is the nonnegative orthant bounded by an *N*-sphere. Under a continuous approximation, as $N \to \infty$, the ultimate shape gain is 1.53dB and the induced signaling distribution on the constituent 1-D constellation becomes half-Gaussian. In practice, the ultimate shape gain can be approached when the 1-D constellation follows a truncated half-Gaussian distribution. We investigate the tradeoffs between shape gain and increases in constellation expansion ratio or peak-to-average power ratio. We compare our shaping results with those for coherent detection systems and direct-detection optical systems with AWGN.**

***Index Terms*—Lattice code, constellation shaping, nonequiprobable signaling, direct detection, shaping gain.**

I. Introduction

A LATTICE code consists of a finite set of points from an N-dimensional lattice Λ (or a translate of Λ) that lie within a finite bounding region $\Re$. Lattice codes for additive white Gaussian noise (AWGN) channels with coherent detection have been explored [1][2] in recent decades. More recently, lattice codes for direct-detection optical systems with AWGN have been studied [3][4].

In lattice codes, the energies associated with different signal points are unequal. In order to minimize average power while maintaining a fixed information bit rate, two commonly used methods are constellation shaping and nonequiprobable signaling [2][5]. Constellation shaping minimizes average signal energy by using a bounding region that encloses a set of minimal-energy points. Under nonequiprobable signaling, signal points of higher energy are chosen less frequently. These two techniques can be applied separately or jointly. Possible drawbacks of shaping and nonequiprobable signaling include increases in peak-to-average power ratio (PAR) and constellation expansion ratio (CER), which reflects the size of the constituent constellation.

From the standpoint of shaping, optical communication systems can be categorized into three groups: coherent detection systems, intensity-modulated direct-detection (IM/DD) systems without optical amplifiers, and IM/DD systems that use optical amplifiers.

Coherent detection, using a phase-locked receiver, has been proposed for fiber and free-space optical systems. Such systems can encode information in complex electric field. With or without optical amplifiers, the dominant noise at the photodetector is usually well-approximated as complex circular Gaussian and signal-independent. One can apply shaping techniques developed for conventional channels [2] without modification.

Optical systems using IM/DD are fundamentally different because the channel output (i.e., detected photocurrent) is nonnegative. Hence, information can be encoded only in the intensity, which is the absolute square of electric field. Some optical systems, such as free-space systems or short-reach fiber systems, use IM/DD without optical amplifiers, and the noise at the photodetector is approximately AWGN. For IM/DD systems with AWGN, shaping has been studied recently [3]. Other optical systems, such as metropolitan and long-haul fiber systems, use IM/DD with optical amplifiers. In the case of IM/DD with amplifiers, the dominant noise at the photodetector is signal-spontaneous beat noise (SSBN), which is signal-dependent. Shaping for this case has not been studied previously, and is the subject of this paper.

The remainder of this paper is organized as follows. In Section II, we describe our modeling of signal and noise in amplified direct-detection (ADD) optical systems. In Section III, we discuss shaping concepts, shaping methods, and derive key shaping results for ADD systems. We give three examples of shaping codes for ADD systems in Section IV. In Section V, we compare and contrast the results of shaping for three types of optical systems mentioned above. In Section VI, we present our summary and conclusions.

II. Amplified Direct-Detection System Model

In an ADD system, an *N*-D signal *X* is formed by transmitting a sequence of *N* time-disjoint 1-D symbols having electric field magnitudes $(x_1, x_2, \cdots, x_N)$, corresponding to intensities $(x_1^2, x_2^2, \cdots, x_N^2)$. In the *i*th symbol interval, $i = 1, \cdots, N$, the field magnitude is drawn from a set of *M* levels:

$$x_i \in \sqrt{I_k}, k = 1, \cdots, M. \quad (1)$$

These *M* field magnitudes correspond to a set of *M* intensity levels $\{I_k, k = 1, \cdots, M\}$.

Paper approved by S. G. Wilson, the Editor for Coding Theory and Applications of the IEEE Communications Society. Manuscript received August 15, 2004; revised January 10, 2006. This research was supported, in part, by National Science Foundation Grant ECS-0335013.

W. Mao is with ArrayComm LLC. 2480 N First Street, Suite 200, San Jose, CA 95131 (e-mail: weimao@arraycomm.com).

J. M. Kahn is with the Department of Electrical Engineering, Stanford University, Stanford, CA 94305 USA (e-mail: jmk@ee.stanford.edu).

Digital Object Identifier 10.1109/TCOMM.2008.040340.

Assuming white noise and negligible intersymbol interference, we can consider the 1-D symbol in one symbol interval, e.g., $t \in [0, T)$. Assuming a rectangular transmitted pulse shape, in this symbol interval, the transmitted field magnitude is expressed as:

$$x(t) = \sqrt{I}, t \in [0, T), \tag{2}$$

corresponding to a transmitted intensity $x^2(t) = I, t \in [0, T)$.

The schematic of an ADD optical receiver is shown in Fig. 1 [6]. The received optical signal passes through an optical amplifier, which has flat gain *G* (W/W) and adds amplified spontaneous emission (ASE) noise $n(t)$ with power spectral density $\frac{N_0}{2}$ (W/Hz). In a well-designed system, the ASE noise is dominant, and other sources of noise (shot noise, thermal noise, etc.) can be ignored [7]. The amplified optical signal is denoted as

$$x_A(t) = \sqrt{G}x(t) + n(t). \tag{3}$$

The optical bandpass filter blocks the ASE noise outside of the signal bandwidth. To simplify our analysis, we use the idealized filter model provided in [8]. The optical filter bandwidth is assumed to be an integral multiple *L* of the signal bandwidth and is denoted as $B_f = L/T$. The overall effect of the optical filter is represented by the impulse response in terms of electric field:

$$h_o(t) = \begin{cases} L/T, & t \in [0, T/L) \\ 0, & \text{otherwise} \end{cases}. \tag{4}$$

The electric field at the output of the optical filter is

$$x_o(t) = x_A(t) \otimes h_o(t). \tag{5}$$

At the bandpass filter output, the optical signal is converted into a photocurrent by a photodetector with responsivity *R* (A/W). The output photocurrent is

$$i(t) = R \cdot x_o^2(t). \tag{6}$$

Following the photodetector, an electrical lowpass filter is used to bandlimit the noise. The electrical filter bandwidth is assumed to be the same as the input signal bandwidth. Following [8], a discrete-time lowpass filter model is used, where the current is sampled and averaged over one symbol duration. The impulse response of the electrical filter is

$$h_e(t) = \frac{1}{L} \cdot \sum_{l=1}^{L} \delta(t - l\frac{T}{L}), \tag{7}$$

and the output to decision device is

$$r = i(t) \otimes h_e(t)\big|_{t=T}. \tag{8}$$

The decision variable *r* is an *L*-th order Chi-square random variable conditioning on input intensity *I*. It can be written as

$$r = R \sum_{l=1}^{L} \left(\sqrt{\frac{GI}{L}} + n_l \right)^2. \tag{9}$$

The n_l are zero-mean i.i.d. Gaussian random variables with variance $\sigma_0^2 = \frac{N_0}{2T}$. The conditional mean and variance of the decision variable are

$$E[r|I] = RGI + \frac{RN_0L}{2T}, \tag{10}$$

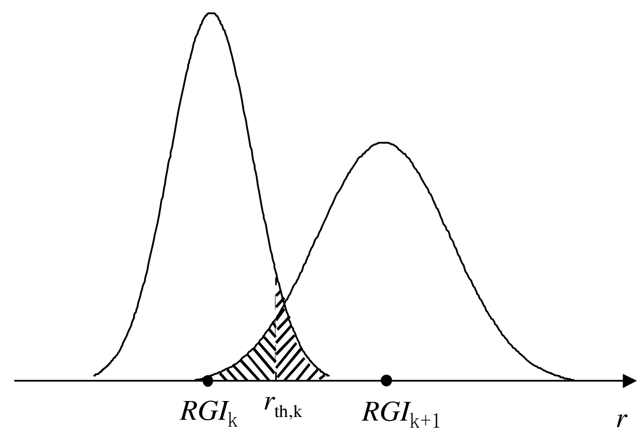

Fig. 2. Conditional probability density functions of photocurrents at neighboring signal levels RGI_k and RGI_{k+1}. The threshold $r_{th,k}$ is set at the geometric mean $RG\sqrt{I_k I_{k+1}}$.

$$\text{VAR}[r|I] = \frac{2R^2GIN_0}{T} + \frac{R^2N_0^2L}{2T^2}. \tag{11}$$

The first term of the mean is from signal. The second term of the mean is from the average power of ASE noise. It introduces a small shift proportional to the optical filter bandwidth and ASE noise power spectral density. The first term of the variance is from signal-ASE beat noise. The second term of the variance is from ASE-ASE beat noise in the optical bandpass filter.

As shown in [9], the received decision variable *r* can be expressed in an alternative form

$$r = R \cdot \left[\left(\sqrt{GI} + N_L \right)^2 + \sum_{i=1}^{L-1} N_i^2 \right], \tag{12}$$

where N_L and N_i are zero-mean i.i.d. Gaussian random variables with variance σ_0^2. We can interpret N_L as the ASE noise within the signal bandwidth and N_i as ASE noises within the optical filter but outside the signal band. It is obvious that signal only beats with ASE noise in the signal band and that in other bands, there is only ASE-ASE beat noise. Therefore, it is desirable to limit the bandwidth of optical filter in order to reduce the amount of ASE-ASE beat noise. However, since the optical filter bandwidth is usually greater than the signal bandwidth in practice, the additional ASE-ASE noise cannot be totally eliminated.

Although it is possible to work with the *L*-th order Chi-square distributed decision variable directly, the solution is usually obtained numerically. We use a first-order Chi-square distribution approximation for the decision variable, which is introduced in [10]:

$$r \approx R \cdot \left[\left(\sqrt{GI + \frac{L-1}{2}\sigma_0^2} + N \right)^2 + \frac{L-1}{2}\sigma_0^2 \right], \tag{13}$$

where *N* is a zero-mean i.i.d. Gaussian random variable with variance σ_0^2. This approximation has the same mean and variance as the original decision variable *r* and is also non-negative. At high signal intensities $GI >> \frac{L-1}{2}\sigma_0^2$, the approximation in (13) is very accurate [6].

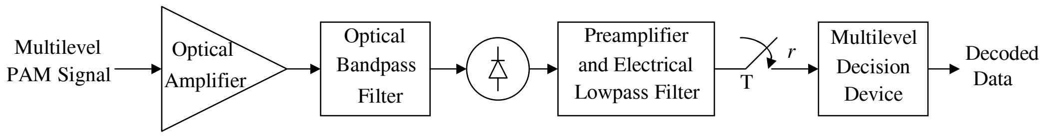

Fig. 1. Schematic of a direct-detection optical receiver with an optical preamplifier.

In order to make the analysis tractable, we will neglect the ASE-ASE beat noise and approximate (13) as Gaussian[1]:

$$r \approx RGI + n, \tag{14}$$

where the signal-spontaneous beat noise $n = 2R\sqrt{GI} \cdot N$ has variance

$$\sigma^2 = (2R^2 GN_0/T) \cdot I, \tag{15}$$

which is proportional to the signal intensity *I*. Thus, conditioned on the intensity level I_k, the decision variable *r* is approximately Gaussian-distributed with mean RGI_k and variance $\sigma_k^2 = (2R^2GN_0/T) \cdot I_k$. A multilevel decision device compares *r* to a set of *M*-1 decision thresholds $\{r_{th,k}, k = 1, \cdots, M-1\}$. We assume that the *k*th threshold is set at the geometric mean of its adjacent levels, i.e., $r_{th,k} = RG\sqrt{I_k I_{k+1}}$, as illustrated in Fig. 2. With this choice of thresholds, the crossover probabilities between neighboring levels become symmetric:

$$\begin{aligned} p_{k\to k+1} &= \frac{1}{2}\text{erfc}(\frac{r_{th,k} - RGI_k}{\sqrt{2}\sigma_k}) \\ = p_{k+1\to k} &= \frac{1}{2}\text{erfc}(\frac{RGI_{k+1} - r_{th,k}}{\sqrt{2}\sigma_{k+1}}), \end{aligned} \tag{16}$$

i.e., the two hashed regions in Fig. 2 are equal in area[2]. We assume an infinite transmitter extinction ratio, i.e., $I_1 = 0$. In order to maintain equal cross-over probabilities at all the thresholds, i.e., $p_{k\to k+1} = p_{k+1\to k} = \frac{1}{2}\text{erfc}(\frac{Q}{\sqrt{2}})$, $k = 1, \cdots, M-1$, the set of signal intensities must form a quadratic series [12][13]:

$$I_k = \frac{2N_0Q^2}{GT} \cdot (k-1)^2, k = 1, \cdots, M. \tag{17}$$

Accordingly, the field magnitudes of 1-D PAM symbols must be chosen from the linear series:

$$\sqrt{I_k} = \sqrt{\frac{2N_0Q^2}{GT}} \cdot (k-1), k = 1, \cdots, M. \tag{18}$$

III. Shaping and Nonequiprobable Signaling

Shaping and nonequiprobable signaling are effective methods to achieve better SNR efficiency given a multidimensional constellation. We will state the fundamental concepts and parameters for ADD signal constellations in Section A. Then in Section B, we will describe the shaping method, the optimal shaping region for ADD signal constellations, and present the induced probability distribution in the constituent 1-D constellation, the ultimate shape gain, and the tradeoffs between shape gain and increases in constellation expansion ratio or peak-to-average power ratio.

A. Concepts and Parameters in ADD Signal Constellations

1) Constellation and Natural Coordinate: In an ADD system, the field magnitudes represent the "natural coordinate system" in which to study shaping for *N*-D ADD signals, since the 1-D symbols form a linear series in field magnitude and each *N*-D signal occupies an equal volume in the *N*-D field magnitude space. For an *N*-D signal $X = (x_1, x_2, \cdots, x_N)$, the *i*th coordinate x_i, $i = 1, \cdots, N$ represents the field magnitude of the *i*th concatenated time-disjoint symbol, whose value is drawn from the set of nonnegative values $\{\sqrt{I_k} = \sqrt{2N_0Q^2/GT}(k-1), k = 1, \cdots, M\}$. Consequently, in the field magnitude coordinate system, the energy of a signal point is represented by its L^2 norm.

An *N*-D ADD signal constellation is a lattice code *C* embedded in an *N*-D vector space with field magnitude coordinates. The signal points are uniformly distributed within the nonnegative orthant bounded by a finite region $\Re$, and occupy equal volumes in *N*-D space. The basic dimension of these signals is 1-D. The average energy of the code $P(C)$ is the average L^2 norm of its *N*-D constellation.

2) Baseline Constellation and Constituent Constellation: A baseline constellation is the basic *N*-D constellation, mostly used for reference and performance comparisons. In 1-D, the PAM constellation is a set of equally spaced points on the nonnegative real line. A baseline constellation is the *N*-time Cartesian product of a PAM constellation with itself (the *N*-D cubic constellation). It is constructed over a simple cubic constellation cornered at the origin with uniform signaling probability mass function.

The constituent 1-D constellation C_1 conveys the range and the distribution of the 1-D symbols. It is defined as the set of all individual coordinate values of all the *N*-D signal points in *C*. It can be obtained by overlapping the projections of the *N*-D constellation onto each coordinate. The induced signaling distribution on constituent 1-D constellation is usually not uniform and can be related directly to the code performance.

3) Normalized Bit Rate, Constellation Figure of Merit, and Shape Gain: Among all the characteristics of an *N*-D constellation *C*, one of the most important is the number of bits that one codeword can represent in *N* dimensions. Suppose signal points are transmitted according to a signaling probability mass function $p(X)$, $X \in C$. The effective number of bits transmitted by the *N*-D symbol is the entropy of

[1] Although the Gaussian approximation follows from the assumption of high signal intensities $GI >> \frac{L-1}{2}\sigma_0^2$, it is reasonably accurate for lower signal intensities [11]. For example, when applied to on-off keying (2-PAM), the Gaussian approximation underestimates the average power required to achieve 10^{-9} bit-error probability by only 0.2 dB [11].

[2] The optimal maximum-likelihood threshold lies at the crossing of the two conditional probability densities shown in Fig. 2, and minimizes the sum $p_{k\to k+1} + p_{k+1\to k}$. Setting the threshold at the geometric mean very nearly minimizes the sum $p_{k\to k+1} + p_{k+1\to k}$, and greatly enhances analytical tractability.

the signaling probability $H(p)$. The normalized bit rate is expressed as:

$$\beta = \frac{1}{N} H(p) = -\frac{1}{N} \cdot \sum_{X \in C} p(X) \log p(X) \qquad (19)$$

per dimension. In many cases when signal points are selected equiprobably, the normalized bit rate is simply $\beta = \frac{1}{N}\log|C|$, where $|C|$ represents the size of the constellation.

Given the normalized bit rate, a common measure for the SNR efficiency of the lattice code is the constellation figure of merit (CFM):

$$\text{CFM}(C) = d^2_{min}(C)/P(C), \qquad (20)$$

where $d^2_{min}(C)$ is the minimum squared distance and $P(C)$ is the average energy per basic dimension. For example, the baseline constellation figure of merit with a normalized bit rate β is $\text{CFM}(C) = 6/(2^\beta - 1)(2^{\beta+1} - 1)$, for $d^2_{min}(C) = 1$. Asymptotically, $\text{CFM}_b(\beta) \approx 3/4^\beta$.

Improvement in SNR efficiency through shaping methods, i.e., the shape gain γ_s, is quantitatively expressed by the ratio of $\text{CFM}(C)$ to its baseline $\text{CFM}_b(\beta)$ (the constellation *C* and its baseline constellation have the same normalized bit rate). Since shaping methods do not change the lattice structure, $d^2_{min}(C)$ is preserved and the shape gain is expressed as:

$$\gamma_s = P_b(\beta)/P(C). \qquad (21)$$

4) Constellation Expansion Ratio and Peak-to-Average Power Ratio: Although shaping and nonequiprobable signaling can help in achieving better SNR efficiency, they both require expansion of the constellation size, which demands wider dynamic range of the transmitter and receiver. Constellation expansion ratio (CER), defined as $\text{CER}(C) = |C_1|/2^\beta$, measures the size change. $|C_1|$ is the size of the constituent 1-D constellation and 2^β is the size of the constituent 1-D constellation of the baseline constellation.

Shaping methods also result in an increase in peak-to-average power ratio (PAR). PAR tends to indicate the sensitivity of a signal constellation to nonlinearities and other signal-dependent perturbations. It is defined as the ratio of the peak energy to the average energy of the constellation.

B. Constellation Shaping and Nonequiprobable Signaling

Constructing an *N*-D constellation on a given *N*-D lattice generally involves choosing the signal points within a bounding region $\Re$ and assigning each point with its signaling probability $p(X)$, $X \in C$ while meeting a certain normalized bit rate. For a fixed lattice, the minimum squared distance is also fixed. In order to achieve good SNR efficiency, the average energy is desired to be as low as possible. A method to assist in constellation point selection and reduce the average energy is shaping, which is choosing a bounding region $\Re$ that includes all the lowest energy points, such that all points within the bounding region have lower energies than the points outside the region. The reduction in average energy through shaping is called shape gain. An alternative method, nonequiprobable signaling, reduces the average energy by assigning higher signaling probabilities to signal points having lower energies. The reduction in average energy through the nonequiprobable

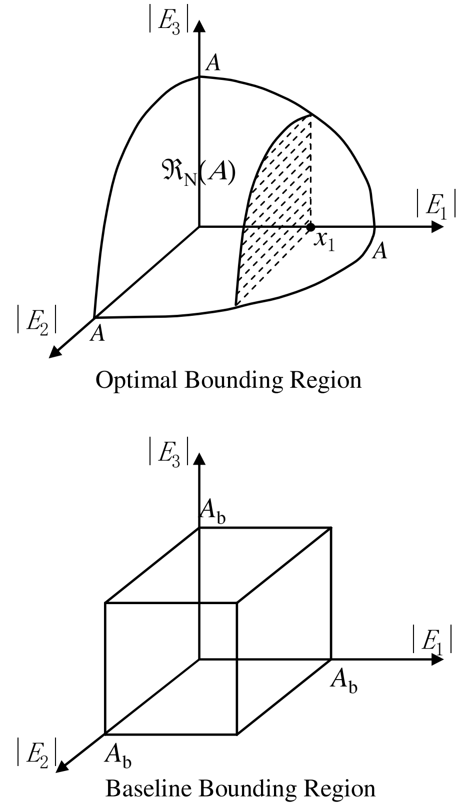

Fig. 3. Optimal bounding region and baseline bounding region.

signaling method is called bias gain. In practice, these two methods are often used jointly. They are jointly referred to as shaping, and the energy gain obtained using both methods is simply referred to as shape gain.

1) Optimal Constellation Bounding Region: The optimal constellation bounding region minimizes the average energy given the number of signal points it must include. Since the L^2 norm represents the energy and the coordinates cannot be negative, the optimal bounding region is the nonnegative orthant bounded by the *N*-sphere $\sum_{i=1}^N x_i^2 = A^2$, where *A* is the highest field magnitude. Points on the surface of the *N*-sphere have the same highest energy A^2. The optimal bounding region is shown In Fig. 3 and is denoted by

$$\Re_N(A) = \left\{ X = (x_1, \cdots, x_N) \middle| \begin{array}{l} x_i \geq 0 \\ \sum_{i=1}^N x_i^2 = A^2 \end{array}, \text{for } i = 1, \cdots, N \right\}. \qquad (22)$$

2) Shape Gain: To calculate the shape gain of a constellation bounded by $\Re_N(A)$ as compared to a baseline constellation, we compare the average energies of the two.

Each lattice point occupies equal unit fundamental volume and has equal signaling probability. When the constellation size is reasonably large, the discrete signal points can be approximated by a uniform continuous distribution within the region $\Re$. Under the continuous approximation, the constellation size is calculated by the volume $V_N(\Re)$ of the continuum bounded by $\Re_N(A)$, which is $1/2^N$ of the N-sphere volume:

$$V_N(\Re) = \begin{cases} \frac{(\sqrt{\pi/2})^{N-1}}{N\cdot(N-2)\cdot\ldots 1}\cdot A^N & (N \text{ odd}) \\ \frac{(\sqrt{\pi/2})^{N}}{N\cdot(N-2)\cdot\ldots 2}\cdot A^N & (N \text{ even}) \end{cases}. \quad (23)$$

The normalized bit rate is $\beta = (\log V_N(\Re))/N$. The average energy per basic dimension is $P(C) = A^2/(N+2)$.

The baseline constellation achieving the same normalized bit rate β is a cubic constellation with peak field magnitude $A_b = [V_N(\Re)]^{1/N}$, which gives the average energy $P_b(\beta) = \frac{A_b^2}{3} = \frac{A^2}{3}\cdot(\frac{V_N(\Re)}{A^N})^{2/N}$. According to (21), the shape gain is:

$$\gamma_s(\Re) = \frac{N+2}{3}\cdot\left(\frac{V_N(\Re)}{A^N}\right)^{2/N}. \quad (24)$$

As the dimensionality goes to infinity, we obtain the ultimate shape gain of $\gamma_s = \frac{\pi}{6}e = 1.53$ dB.

3) Induced Signaling Distribution in Constituent 1-D Constellation: Throughout the shape gain calculations above, we have assumed that the signaling probability distribution on the $2^{N\beta}$ points in the optimal bounding region is uniform. However, the induced probability distribution in the constituent 1-D constellation is not necessarily uniform. In fact, with the bounding region $\Re_N(A)$, the projection of the N-D constellation onto its constituent 1-D constellation shows that points in the constituent constellation with lower energies are used more frequently than those with higher energies.

The induced probability distribution $p_{in}(x_1)$ on the first coordinate x_1 is proportional to the volume $V_{N-1}(\Re)$ of the (N-1)-sphere centered at x_1 (see the slashed area in Fig. 3), i.e.,

$$p_{in}(x_1) \propto \frac{V_{N-1}\left(\Re_{N-1}(\sqrt{A^2-x_1^2})\right)}{V_{N-1}\left(\Re_{N-1}(A)\right)} = \left(\sqrt{1-\frac{x_1^2}{A^2}}\right)^{N-1}. \quad (25)$$

Note that the average energy of the constituent 1-D constellation with signaling probability $p_{in}(x_1)$ remains the same as the original constellation. Recall the expression for the average energy and substitute A^2 by $(N+2)\cdot P(C)$. Then the induced probability distribution becomes $\left(1-\frac{x_1^2}{(N+2)P(C)}\right)^{\frac{N-1}{2}}$. As $N\to\infty$,

$$p_{in}(x_1) \propto \lim_{N\to\infty}\left(1-\frac{x_1^2}{(N+2)\cdot P(C)}\right)^{\frac{N-1}{2}} = \exp\left\{-\frac{x_1^2}{2P(C)}\right\}, \text{for } x_1 \geq 0. \quad (26)$$

The induced probability distribution in the constituent 1-D constellation is half-Gaussian [14][15]. From the perspective of shaping methods, the constituent 1-D constellation employs nonequiprobable signaling, i.e., it chooses more frequently signal points that lie close to the origin. The above example shows that bounding region shaping results in nonequiprobable signaling on the constituent 1-D constellation. Therefore, bounding region shaping and nonequiprobable signaling are often designed jointly, and no particular effort is made to distinguish between the two methods. The induced probability distribution on the 1-D constellation gives a normalized bit rate of $\beta = H(p_{in}) = \frac{1}{2}\log(\frac{\pi e}{2}P)$. The 1-D baseline constellation with the same normalized bit rate has the constellation size 2^β and the average energy $\frac{1}{3}\left(\sqrt{\frac{\pi e}{2}P}\right)^2 = \frac{\pi e}{6}P$. It yields the same shape gain result from the perspective of the constituent 1-D constellation.

TABLE I
SHAPE GAINS, CONSTELLATION EXPANSION RATIOS, AND PEAK-TO-AVERAGE POWER RATIOS FOR N-DIMENSIONAL CONSTELLATIONS WITH OPTIMAL BOUNDING REGIONS

N	γ_s in dB	CER	PAR
1	0	1	3
2	0.20	1.13	4
3	0.35	1.24	5
5	0.54	1.43	7
8	0.73	1.68	10
16	0.98	2.19	18
32	1.17	2.94	34
64	1.31	4.04	66

4) Shape Gain vs. CER and PAR: Shaping and nonequiprobable signaling favor signal points with less energies, which directly results in the expansion of the constituent 1-D constellation size. Improvements in the SNR efficiency are achieved at the expense of an increased peak-to-average power ratio. For the N-D constellation with optimal bounding region $\Re_N(A)$, the shape gain, constellation expansion ratio and peak-to-average power ratio are

$$\begin{aligned} \gamma_s(\Re) &= \frac{N+2}{3}\cdot\left(\frac{V_N(\Re)}{A^N}\right)^{2/N}, \\ \text{CER} &= \frac{A}{A_b} = \frac{A}{V_N(\Re)^{1/N}}, \\ \text{PAR} &= \frac{A^2}{P(C)} = N+2 = 3\cdot\gamma_s(\Re)\cdot\text{CER}^2. \end{aligned} \quad (27)$$

Design of an N-D constellation demands a shape gain as close to that of the optimal bounding region as possible, while maintaining reasonable constituent constellation size, peak-to-average power ratio, and implementation complexity. Table 1 lists the shape gain, CER, and PAR for different numbers of constellation dimensions. No shaping is involved in designing a 1-D constellation. Consequently, when $N = 1$, there is no shape gain and the constellation expansion ratio is kept at 1. As the constellation dimension N increases, the shape gain improves at the price of a linear increase in peak-to-average power ratio as well as increased constellation expansion ratio. For $N = 8$, about half of the ultimate shape gain (0.73 dB) can be achieved.

Achieving the ultimate shape gain requires the half-Gaussian induced 1-D distribution, which has infinite peak energy, making its implementation impractical. Consider a peak-energy-limited constituent 1-D constellation with its induced 1-D distribution $p_{in}(x_1)$ bounded within the region $[0, A]$. Denote the differential entropy and the second moment (which is equivalent to the average energy) of $p_{in}(x_1)$ by H and P, respectively. Then the shape gain, the constellation expansion ratio and the peak-to-average power ratio can be expressed in

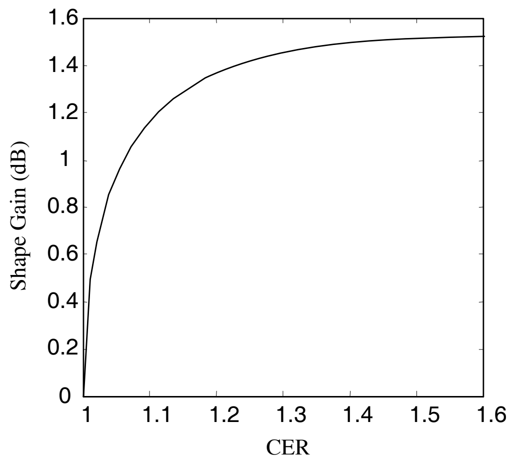

Fig. 4. Best possible tradeoff between shape gain $\gamma_s(\Re)$ and constellation expansion ratio (CER).

terms of H and P:

$$\begin{aligned} \gamma_s(\Re) &= \frac{(2^H)^2}{3P}, \\ \text{CER} &= \frac{A}{2^H}, \\ \text{PAR} &= \frac{A^2}{P} = 3 \cdot \gamma_s(\Re) \cdot \text{CER}^2. \end{aligned} \tag{28}$$

By standard variational arguments with a Lagrange multiplier λ, the distribution that maximizes the entropy H given a certain second moment P is a truncated half-Gaussian distribution.

$$p^*_{in}(x_1) = \begin{cases} K(\lambda) \cdot \exp\Big(-\frac{\lambda x_1^2}{A^2}\Big), & 0 \le x_1 \le A \\ 0, & \text{otherwise} \end{cases}, \tag{29}$$

where λ is a parameter that governs the tradeoff between H and P as well as the tradeoff between γ_s and CER, and $K(\lambda)$ is a function of λ that normalizes the probability distribution $p^*_{in}(x_1)$. When $\lambda = 0$, $p^*_{in}(x_1)$ is uniform over the region $[0, A]$ and zero elsewhere, $\gamma_s = 1 = 0$ dB, CER =1, and PAR=3, which is the same as those of a baseline constellation. As the value of λ gets larger, the variance of the half-Gaussian distribution becomes smaller and the truncated portion becomes negligible compared to the entire half-Gaussian distribution. Therefore, the distribution $p^*_{in}(x_1)$ can be approximated by the half-Gaussian distribution and the shape gain approaches the ultimate limit asymptotically at the expense of increasing CER and PAR.

We use numerical integration to compute $K(\lambda)$, H, and P, varying λ between 0 and 6. In Fig. 4 and Fig. 5, we plot the best tradeoff between γ_s and CER and between γ_s and PAR, respectively. In principle, 1.3 dB shape gain can be achieved if CER = 1.15 and PAR = 5.5 are allowed. If the tolerance of CER increases to 1.45 and that of PAR increases to 9, the shape gain can be as high as 1.5 dB, which is 98% of the ultimate shape gain.

IV. Shaping Code Examples

The analysis above is based on a continuous approximation of the signal constellation. To illustrate how the theory is applied to practical discrete constellations, we will give the following three shaping codes as examples. In Section A, we present a 1-D four-level PAM constellation with signaling probability derived from the truncated half-Gaussian distribution. In Section B, we present an 8-point constellation obtained through shaping a 2-D 3-PAM cubic constellation. In Section C, we present a practical application of shaping to Schlafli lattice D_4.

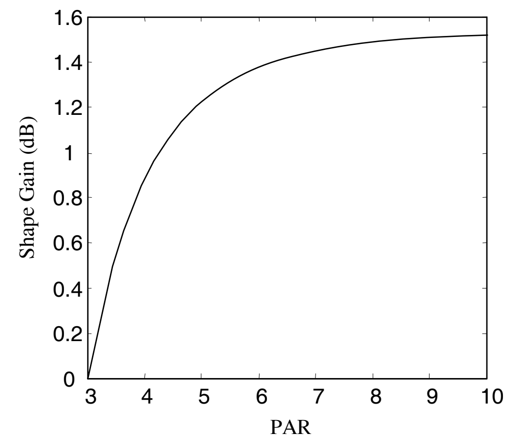

Fig. 5. Best possible tradeoff between shape gain $\gamma_s(\Re)$ and peak-to-average power ratio (PAR).

TABLE II
Huffman Code for the 4-Level PAM Constellation

Source Bits	Constellation Point	A Priori Probability
0	0	1/2
10	1	1/4
110	2	1/8
111	3	1/8

A. Constituent 1-D 4-PAM Constellation

We will construct a 4-level PAM constellation with a goal of achieving at least 1 dB shape gain at a bit rate of approximately 2 bits per dimension while keeping reasonable CER and PAR.

We begin with a basic 4-level PAM constellaton that is uniformly spaced in field magnitude. From the expression of the truncated half-Gaussian distribution (29), the tradeoff parameter λ must be at least 1.5 if the desired shape gain is 1 dB. We set $\lambda = 1.5$, $A = 3$, and take values at points $(0, 1, 2, 3)$. We obtain a probability distribution that is a discrete approximation of the truncated half-Gaussian distribution $p_{4-PAM} = (0.387, 0.328, 0.199, 0.086)$. We then use a binary Huffman code to map the source bit sequences to the constellation points and round the probabilities to dyadic numbers. Table 2 shows a simple Huffman code for the 4-level PAM constellation. Note that Huffman codes do not guarantee a constant symbol rate. The normalized bit rate and the average energy of this shaping code are $\beta = 1.829$ bits per dimension and $P = 1.900$, respectively.

The shape gain is calculated by comparing the constellation average energy to that of a baseline constellation with the same normalized bit rate and the same bit error rate. However, in this shaping code, the normalized bit rate is a fractional number

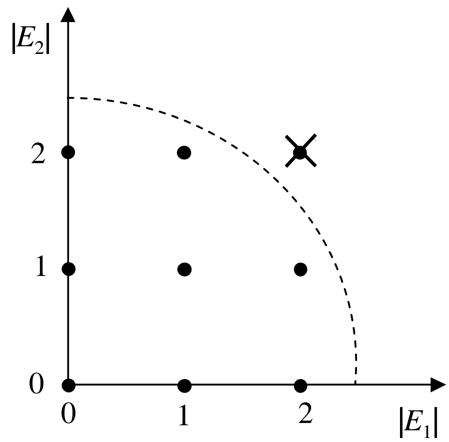

Fig. 6. Two-dimensional eight-point constellation obtained by shaping a two-dimensional 3-PAM baseline constellation. The dashed line indicates the constellation bounding region.

and the baseline constellation is not directly identifiable. Suppose the shaping code is transmitted at unit symbol rate. Consider a 4-level baseline constellation with field magnitude scaled down by a factor of α, transmitted at a symbol rate $\beta/2$, such that this baseline constellation has the same normalized bit rate as our shaping code. To maintain the same bit-error probability, the cross-over probability (16) needs to be kept constant, i.e., I_k/σ_k remains the same. The signal strength I_k increases with α^2. The noise variance σ_k^2 is proportional to both I_k and the symbol rate $1/T$. Hence, α should be equal to $\sqrt{\beta/2} = 0.956$. The average energy of this baseline constellation is 3.195. Therefore, the shape gain of the 4-level PAM constellation is $\gamma_s = \frac{3.195}{1.900} = 1.682 = 2.26$ dB. This value is significantly above the ultimate shape gain based on the continuous approximation. This example illustrates that small, discrete consellations can yield shape gains that deviate significantly from the ultimate shape gain. The constellation expansion ratio and the peak-to-average power ratio are 1.13 and 4.7, respectively.

B. 2-D 3-PAM Constellation with 8-points

This example code is an application of constellation bounding region shaping with equiprobable signaling. We start with a 2-D 3-PAM baseline constellation. As shown in Fig. 6, the 2-D circular optimal bounding region omits the point with highest energy and yields the 2-D 8-point constellation with equiprobable points. Suppose the source bit sequence is segmented into 3 bits per symbol. The 8 distinct symbols and the 8 points in the constellation permit a one-to-one mapping. The normalized bit rate and the average energy per dimension are $\beta = 1.5$ bits per 1-D and $P = 1.375$, respectively. The constituent baseline constellation is obtained from scaling a 1-D 3-PAM baseline constellation by a factor $\alpha = \beta/(\log_2 3) = 0.973$ and transmitting the symbols at the rate $\beta/(\log_2 3)$. Such a baseline constellation yields an average energy of 1.577 per dimension. Therefore, the shape gain, the constellation expansion ratio, and the peak-to-average energy ratio are $\gamma_s = 1.147 = 0.60$ dB, CER=1.06, and PAR=1.82, respectively.

C. 4-D Constellations based on Schlafli Lattice D_4

The Schilafli lattice D_4 is the set of integer-valued 4-tuples whose sum of coordinates is even. It is defined by the generating matrix

$$D_4 = \begin{bmatrix} 2 & 0 & 0 & 0 \\ 1 & 0 & 0 & 1 \\ 0 & 1 & 0 & 1 \\ 0 & 0 & 1 & 1 \end{bmatrix}, \qquad (30)$$

The D_4 lattice points are described by $x = uD_4$, where the components of the 1×4 vector u are integer valued.

In the nonnegative orthant of D_4 lattice, there are 1 point with zero energy, 6 points with energy equal to 2, 5 points with energy equal to 4, and 12 points with energy equal to 6. We take all the 12 points with energy less than 6 and any 4 points of energy 6 to form a 16-point constellation on D_4 lattice. This constellation has normalized bit rate $\beta = 1$ bit per 1-D and average energy $P = 0.875$ per 1-D. Points in this constellation have minimum Euclidean distance of $\sqrt{2}$. The constituent baseline constellation is obtained from scaling a binary baseline constellation by a factor $\alpha = \sqrt{2}$. Such a baseline constellation yields an average energy of 1 per dimension. Therefore, the shape gain, the constellation expansion ratio, and the peak-to-average energy ratio are $\gamma_s = 1.143 = 0.58$ dB, CER=1.5, and PAR=1.72, respectively.

V. Comparison of Shaping in Optical Systems

In Section I, optical systems have been categorized into three groups with respect to information encoding methods and noise properties. Systems using coherent detection modulate electric field to encode information, while direct-detection systems modulate intensity. Among direct-detection systems, those without amplifiers are usually dominated by AWGN, while those with amplifiers are dominated by signal-spontaneous beat noise.

Table 3 shows some major properties of shaping in those three types of optical systems. First, because of their different signal and noise characteristics, the three types of systems have different natural coordinates and different constituent constellation dimensions. Coherent systems use both inphase and the quadrature field components to transmit information. Those two field components are transmitted and received simultaneously, therefore, are generally described as a doublet. Hence, the constituent constellation of the coherent systems is 2-D with electric fields $E_i, i = 1, 2$ as coordinates. The direct-detection systems transmit information only through field intensity variations, so their constituent constellations are 1-D. Due to the differences in signal dependence of noise, the two groups of direct-detection systems have their signals designed as uniformly distributed and quadratically distributed in field intensity, respectively. The direct-detection systems with AWGN naturally have the field intensity I as coordinate. The amplified direct-detection systems have the field magnitude as coordinate to preserve the uniformity of its lattice.

The energy representations are a direct consequence of the choice of natural coordinates in each type of system. The signal energies in coherent systems and ADD systems

TABLE III
COMPARISON OF SHAPING IN VARIOUS OPTICAL SYSTEMS. THE PARAMETER A IS THE PEAK FIELD MAGNITUDE.

	Coherent Detection with AWGN	Direct Detection with AWGN	Direct Detection with Signal-Spontaneous Beat Noise
Constituent Constellation	2-D constellation with electric fields $E_i, i = 1, 2$ as coordinates	1-D constellation with field intensity $I = \lvert E \rvert^2$ as coordinate	1-D constellation with field magnitude $\lvert E \rvert$ as coordinate
Baseline Constellation	Simple N-D cubic lattice with cubic-shaped bounding region centered at the origin	Simple N-D cubic lattice with cubic-shaped bounding region cornered at the origin	Simple N-D cubic lattice with cubic-shaped bounding region cornered at the origin
Energy	L^2 norm	L^1 norm	L^2 norm
Average Energy of the Baseline Constellation	$P = \frac{2A^2}{3}$ per 2-D	$P = \frac{A^2}{2}$ per 1-D	$P = \frac{A^2}{3}$ per 1-D
Optimal Shaping Region	N-sphere centered at the origin 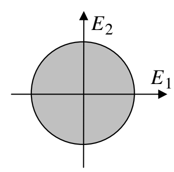	Nonnegative orthant bounded by N-simplex 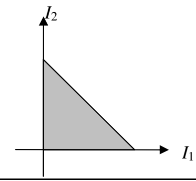	Nonnegative orthant bounded by N-sphere 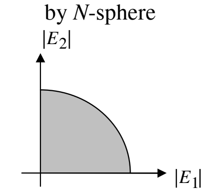
Average Energy Under Optimal Shaping Region	$P = \frac{A^2}{(N/2+1)}$ per 2-D	$P = \frac{A^2}{(N+1)}$ per 1-D	$P = \frac{A^2}{(N+2)}$ per 1-D
Induced Optimal Signaling Distribution in Constituent Constellation	$p(E) = \frac{1}{\pi P} \exp\left(-\frac{\lvert E \rvert^2}{P} \right)$, $E = (E_1, E_2)$ 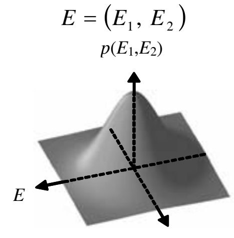	$p(I) = \frac{1}{P} \exp\left(-\frac{I}{P} \right)$, $I \geq 0$ 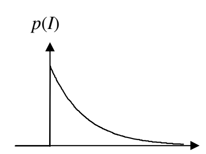	$p(\lvert E \rvert) = \sqrt{\frac{2}{\pi P}} \exp\left(-\frac{\lvert E \rvert^2}{2P} \right)$, $\lvert E \rvert \geq 0$ 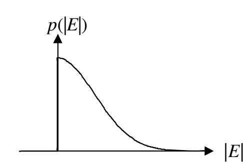
Ultimate Shape Gain	$\pi e/6 = 1.53$ dB	$e/2 = 1.33$ dB	$\pi e/6 = 1.53$ dB

are both represented as the L^2 norm, which leads to many similarities in shaping results of those two system types. Both of their optimal shaping regions are bounded by N-spheres, except that the constellation of ADD systems occupies only the nonnegative orthant. Their induced signaling distributions are Gaussian and half-Gaussian, respectively, which leads to identical ultimate shape gains of 1.53 dB in both system types. Under the continuous approximation, the total energies in both system types are the same with the same peak field amplitude[3], but the average energy in coherent systems is exactly twice the average energy of ADD systems. This is only because the basic dimension in coherent detection systems is two and that in ADD systems is one.

Both the field intensity and the field magnitude are nonnegative. Therefore, the constellations of direct-detection systems both without and with amplifiers are constrained to lie in the nonnegative orthant. These two types of systems share similar baseline constellations. Although both system types encode information in field intensities, their dramatically different energy represention make their optimal shaping regions, their induced optimal signaling distributions, and their shaping gains differ significantly. However, if we were to choose field intensity as the coordinate for ADD systems, the optimal bounding region would become the nonnegative orthant bounded by N-simplex, the same as in direct-detection systems with AWGN.

[3]Peak field amplitude refers to the peak amplitudes of both $E_i, i = 1, 2$ in coherent systems and the peak amplitude of $|E|$ in ADD systems.

VI. CONCLUSION

In amplified direct-detection systems, the dominant noise is signal-spontaneous beat noise, whose variance is proportional to the signal intensity. Consequently, the signal points in ADD systems are designed to be quadratically distributed in intensity to ensure equal cross-over probabilities. In order to define a uniform lattice of signal points, field magnitudes represent the natural coordinate system. In such a framework, the signal energy is represented by L^2 norm and the optimal constellation bounding region is the nonnegative orthant bounded by N-sphere. As $N \to \infty$, the ultimate shape gain under a continuous approximation is 1.53 dB, and the induced signaling distribution on the constituent 1-D constellation becomes half-Gaussian. The ultimate shape gain can also be approached by using a truncated half-Gaussian induced 1-D distribution. Tradeoffs between the shape gain and negative effects, i.e., constellation expansion ratio and peak-to-average power ratio have been investigated. In theory, 98% of the ultimate shape gain can be achieved at the cost of increasing CER to 1.45 and PAR to 9. Example shaping codes have been developed, which showed that the shape gain in small discrete PAM constellations can significantly exceed the ultimate shape gain derived under a continuous approximation.

Comparison of coherent-detection systems and direct-detection systems with and without amplifiers showed that shaping results in ADD systems are very similar to those of coherent detection systems, because energy is represented as an L^2 norm in both types of systems. By contrast, although direct-detection systems with and without amplifiers employ the same detection scheme, their different signal distributions lead to significantly different shaping results.

REFERENCES

[1] G. D. Forney, "Coset codes-part I: introduction and geometrical classification," *IEEE Trans. Inform. Theory*, vol. 34, pp. 1123-1151, Sept. 1988.

[2] G. D. Forney and L. Wei, "Multidimensional constellations-part I: introduction, figures of merit, and generalized cross constellations," *IEEE J. Select. Areas Commun.*, vol. 7, pp. 941-958, Aug. 1989.

[3] D. Shiu and J. M. Kahn, "Shaping and nonequiprobable signaling for intensity-modulated signals," *IEEE Trans. Inform. Theory*, vol. 45, pp. 2661-2668, Nov. 1999.

[4] S. Hranilovic and F. R. Kschischang, "Optical intensity-modulated direct detection channels: signal space and lattice codes," *IEEE Trans. Inform. Theory*, vol. 49, pp. 1385-1399, June 2003.

[5] A. R. Calderbank and L. H. Ozarow, "Nonequiprobable signaling on the Gaussian channel," *IEEE Trans. Inform. Theory*, vol. 36, pp. 726-740, July 1990.

[6] R. You and J. M. Kahn, "Coded modulation techniques for direct-detection optical fiber communication systems with optical amplifiers," submitted to *IEEE Trans. Commun.*, Mar. 2003.

[7] G. P. Agrawal, *Fiber-Optic Communication Systems*, Third Edition. John Wiley and Sons, 2002.

[8] O. K. Tonguz and L. G. Kazovky, "Theory of direct-detection lightwave receivers using optical amplifiers," *J. Lightwave Technol.*, vol. 9, no. 2, pp. 174-181, Feb. 1991.

[9] H. O. Lancaster, *The Chi-Squared Distribution*. John Wiley and Sons, Inc., 1969.

[10] M. Sankaran, "Approximations to the non-central chi-square distribution," *Biometrika*, vol. 50, pp. 199-204, June 1963.

[11] J. M. Kahn and K.-P. Ho, "Spectral efficiency limits and modulation/detection techniques for DWDM systems," *IEEE. J. Select. Topics Quantum Electron.*, vol. 10, no. 2, pp. 259-272, Mar./Apr. 2004.

[12] S. Walklin and J. Conradi, "Multilevel signaling for increasing the reach of 10 Gb/s lightwave systems," *J. Lightwave Technol.*, vol. 17, pp. 2235-2248, Nov. 1999.

[13] J. L. Rebola and A. Cartaxo, "Optimization of level spacing in quaternary optical communication systems," in *Proc. SPIE Applications of Photonic Technology*, Quebec City, Canada, June 2000, vol. 4087, pp. 49-59.

[14] A. Mecozzi and M. Shtaif, "On the capacity of intensity-modulated systems using optical amplifiers," *IEEE Photon. Technol. Lett.*, vol. 13, no. 9, pp. 1029-1031, Sept. 2001.

[15] K.-P. Ho, "Exact evalutation of the capacity for intensity-modulated direct-detection channels with optical amplifier noises," *IEEE Photon. Technol. Lett.*, vol. 17, no. 4, pp. 858-860, Apr. 2005.

Wei Mao received the B.A. degree in Physics, the M.S. and Ph.D. degrees in Electrical Engineering from U.C. Berkeley in 1998, 2001, and 2005, respectively. She is currently working as a systems research engineer at ArrayComm LLC. Her current research interests include various topics in MIMO wireless communications.

Joseph M. Kahn received the A.B., M.A. and Ph.D. degrees in Physics from U.C. Berkeley in 1981, 1983 and 1986, respectively. From 1987-1990, he was at AT&T Bell Laboratories, Crawford Hill Laboratory, in Holmdel, NJ. He demonstrated multi-Gb/s coherent optical fiber transmission systems, setting world records for receiver sensitivity. From 1990-2003, he was on the faculty of the Department of Electrical Engineering and Computer Sciences at U.C. Berkeley, performing research on optical and wireless communications. Since 2003, he has been a Professor of Electrical Engineering at Stanford University. His current research interests include single- and multi-mode optical fiber communications, free-space optical communications, and MEMS for optical communications. Professor Kahn received the National Science Foundation Presidential Young Investigator Award in 1991. He is a Fellow of the IEEE. From 1993-2000, he served as a Technical Editor of *IEEE Personal Communications Magazine*. In 2000, he helped found StrataLight Communications, where he served as Chief Scientist from 2000-2003.